Scientific Research Publishing

Open Journal of Applied Sciences, 2026, 16(11), 4547-4558
https://www.scirp.org/journal/ojapps
ISSN Online: 2165-3925
ISSN Print: 2165-3917

Electric Arc Plasma Electroconsolidation for the Manufacture of Clay-Ash-Sand Composite Materials

Ayi Kévin Ajavon[1*], Diyakadola Dihéénane Bafai[1], Kékéli Codjo Maurille Aziade[1], Ablam Lazare Afanou[1], Bassaï Magnoudéwa Bodjona[1], Sama Ouro[2], Gado Tchangbedji[1]

[1]Laboratoire de Gestion, Traitement et Valorisation des Déchets (GTVD), Faculty of Sciences, University of Lomé, Lomé, Togo
[2]Centre Régional de Formation pour l'Entretien Routier (CERFER), Lomé, Togo
Email: *ajavonayikevinmail@gmail.com

How to cite this paper: Ajavon, A.K., Bafai, D.D., Aziade, K.C.M., Afanou, A.L., Bodjona, B.M., Ouro, S. and Tchangbedji, G. (2026) Electric Arc Plasma Electroconsolidation for the Manufacture of Clay-Ash-Sand Composite Materials. *Open Journal of Applied Sciences*, **16**, 4547-4558.
https://doi.org/10.4236/ojapps.2026.1611249

Received: August 27, 2026
Accepted: November 17, 2026
Published: November 20, 2026

Copyright © 2026 by author(s) and Scientific Research Publishing Inc.
This work is licensed under the Creative Commons Attribution International License (CC BY 4.0).
http://creativecommons.org/licenses/by/4.0/

Open Access

Abstract

Electroconsolidation is a process that involves injecting a sufficient quantity of ions (binder) into clay soil using a chemical solution and then using an electric current to cause these ions to migrate through the soil in order to irreversibly stabilize it. This method of consolidating clay soils—which requires the use of chemical solutions whose ions or combination of ions, form a binder—could have several potential applications in the field of construction materials if it could be optimized by replacing the chemical solution (source of ions) and direct current with an electric arc plasma. It is within this context that this study was conducted, with the goal of developing eco-friendly bricks made from clay, wood ash (industrial waste), and sand using an electric arc plasma-assisted consolidation process. The materials were developed using two approaches. The first approach involves consolidating a mixture of raw material powders (sand, ash, clay) by directly bombarding the mixture with electric arc plasma. The second approach, meanwhile, involves consolidating blocks composed of varying proportions of a mixture of raw materials (sand, ash, clay, and an organic binder) using electric arc plasma. The results of the physicochemical and mineralogical characterizations of the clay (kaolinite), wood ash (70% calcium oxide), and sand (95% silica) confirmed the decision to use them in the production of eco-friendly bricks. The results of the physicochemical characterization of the materials obtained through the first approach revealed, compared to the raw materials, a high iron oxide content in the materials derived from the ash-clay (more than 4%) and clay-sand (more than 8%) mixtures, whereas the material derived from the ash-sand mixture had a high alumina content of more than 10%. This increase in metal oxide confirms, on the one hand, the solubilization of a portion of the metal elec-

trodes within the plasma phase and, on the other hand, that the electric arc plasma can be used as both a source and a means of transporting ions. Microscopic analysis of the materials obtained in the first experiment shows that they have a glassy, amorphous surface. The results of the compressive strength of the materials obtained using the second consolidation method suggest satisfactory structural homogeneity and a selective structural affinity of the plasma consolidation process toward sand-rich matrices compared to clay-rich matrices. Thus, for sand contents ranging from 95% to 0%, compressive strengths ranging from 30.27 ± 0.91 MPa to 14.4 ± 0.23 MPa, respectively, were obtained. These results show that it is therefore possible to manufacture eco-friendly bricks from ash, clay, and sand using only the electric arc plasma-assisted electroconsolidation process.

Keywords

Clay, Wood Ash, Sand, Electroconsolidation, Electric Arc Plasma, Eco-Friendly Bricks

1. Introduction

The construction sector is one of the world's largest emitters of greenhouse gases. It represents approximately 37% of global CO_2 emissions related to the production of materials [1]. Among these materials, baked clay bricks are in high demand worldwide. However, the traditional manufacturing process requires baking the clay at very high temperatures (900˚C), which consumes enormous amounts of fossil fuels and emits significant amounts of CO_2, without taking into account the depletion of clay resources. A study conducted in Madagascar showed that artisanal production of one metric ton of baked clay bricks can generate up to 555 kg of CO_2 [2].

Added to this is the production of Portland cement, which is used as a binder in concrete and cinder blocks. Cement manufacturing represents approximately 8% of global CO_2 emissions, or more than 2.5 billion metric tons per year [3]. This carbon footprint results both from the chemical decarbonation of limestone and from the use of fossil fuels in rotary kilns at temperatures of 1450˚C and higher [4]. The cement industry has thus become the third-largest emitter of greenhouse gases in the world, behind China and the United States [5].

Given the climate emergency, the ever-increasing demand for affordable materials, and the depletion of natural resources, it is imperative to review and rethink the design processes for these materials.

The current challenge, therefore, is to develop new environmentally friendly materials capable of combining a low carbon footprint (no firing, low-temperature firing, or eco-friendly binders); the use of local waste (industrial, agricultural, or construction waste) to partially replace clay or sand [6]; and thermal and mechanical performance that meets modern building standards (strength, porosity, thermal conductivity, and sound insulation).

Our research is conducted within this context. Our goal is to develop and implement new, environmentally friendly brick-making techniques by exploring the innovative approach of electric arc plasma electroconsolidation.

More specifically, this study aims to characterize the raw materials, produce briquettes using electroconsolidation, and investigate the physicochemical and mechanical properties of the resulting materials.

2. Materials and Methods

2.1. Pre-Processing of Raw Materials

2.1.1. Afagnan Clay

The clay was collected in Afagnan (6˚29'39"N, 1˚37'56"E), a town located in southern Togo, 95 km from Lomé. The sample was collected at a depth of 18 m. The clay sample was dried for 96 hours, crushed, ground, and sieved to 105 µm to obtain a fine clay powder.

2.1.2. Ash

The ash comes from eucalyptus wood used as fuel in the furnace at the SOPAL vegetable oil refinery, located in the Lomé port area. Once collected, the ash was sifted to 75 µm and then dried in an oven at a temperature of 105˚C during 24 hours.

2.1.3. Sand

The sand (Figure 1) was collected at the University of Lomé, specifically behind the GTVD laboratory. Once collected, the sand was sieved using a 1-mm mesh sieve to remove waste.



Figure 1. Image of sand used as raw material.

2.2. Electric Arc Plasma Operating Device

The operating system consists of a generator, a ZVS driver, and a flyback transformer (Figure 2). The generator's role is to supply a DC voltage to the ZVS driver, which converts this DC voltage into a pulse that the flyback transformer then amplifies to a high voltage (50 kV) in order to generate an electric arc plasma between its output electrodes [7].

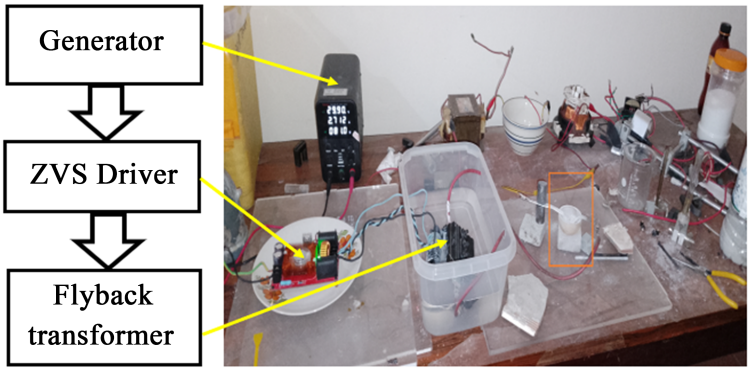


Figure 2. Image of the electric arc plasma operating device.

2.3. Electroconsolidation and Materials Manufacturing

Two different approaches were used in the design of the materials.

2.3.1. First Approach

The process begins by immersing the flyback transformer electrodes in mixtures of ash powder, clay, and sand, followed by the activation of the electric arc plasma while maintaining the generator power at a minimum of 100 W for 15 minutes (Figure 3). The experiment was conducted at room temperature (25˚C) and at an atmospheric pressure of 1 atm in an alumina crucible.

To better understand the various interactions between the raw materials (ash, sand, and clay), the electrodes, and the plasma, three types of materials were produced by bombarding equiproportional mixtures of ash-sand, ash-clay, and sand-clay while varying the type of electrodes. For the first experiment, aluminum and iron electrodes were used.

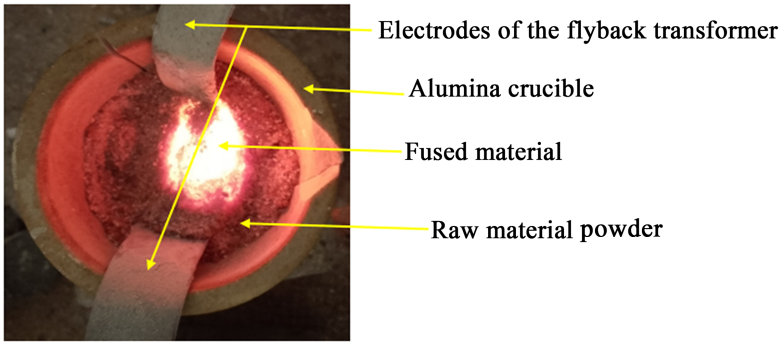


Figure 3. Image illustrating electroconsolidation according to the first approach.

2.3.2. Second Approach

In general, the process involves exposing 64 cm^3 cubic sample blocks to an arc plasma generated by aluminum electrodes for 45 minutes. The distance between each electrode and the sample is 1 cm. These blocks composed of a measured mixture of clay, ash, and sand, combined with an average mass of 10 g of a soy lecithin solution with a concentration of 2 g/mL, which serves as an organic binder (Figure 4). The average mass of the sample blocks is 200 g. The power consumption

during the experiment was 100 W. The experiment was conducted at room temperature (25˚C) and at an atmospheric pressure of 1 atm. As part of a more in-depth study, different proportions were used in the mixtures to determine the optimal formulations (Table 1).

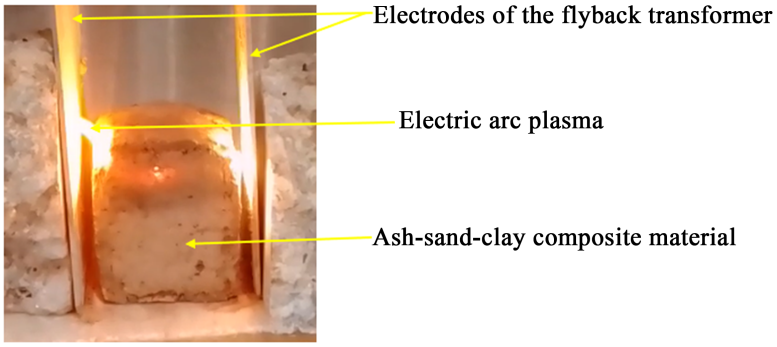


Figure 4. Image annotated illustrating electroconsolidation according to the second approach.

Table 1. Details regarding the various proportions of powders used in the consolidation of materials according to the second approach.

	M1	M2	M3	M4	M5	M6	M7	M8	M9	M10	M11	M12	M13	M14	M15	M16	M17	M18
X1: Mass percentage of clay	82	72	62	57	57	57	57	95	30.33	22	27.77	22	13.67	13.67	5.33	13.67	13.67	0
X2: Mass percentage of sand	4	9	14	14	9	4	0	0	32.33	49	52.85	57.33	65.67	57.33	57.33	79.33	74	95
X3: Mass percentage of ash	9	14	19	24	29	34	38	0	32.34	24	14.38	15.67	15.66	24	32.34	2	7.33	0
X4: Mass percentage of lecithin	5	5	5	5	5	5	5	5	5	5	5	5	5	5	5	5	5	5

3. Characterization Techniques and Results

3.1. Characterization of Raw Materials

To characterize the raw materials, an elemental analysis using X-ray fluorescence (XRF) spectroscopy was performed on the ash (Table 2) and sand (Table 3) to determine their elemental chemical composition. The same analysis, along with X-ray diffraction (XRD), was performed on the clay to determine its chemical composition (Table 4) and mineralogical composition (Figure 5).

Table 2. Elemental chemical composition of the ash.

Mass percentage (%)	SiO_2	Al_2O_3	CaO	MgO	Na_2O	K_2O	Fe_2O_3	TiO_2	Mn_2O_3	P_2O_5	BaO	SO_3	LOI
Ash	2.97	0.75	70.11	7.50	0.37	6.70	0.71	0.15	0.21	2.61	0.24	2.55	5.13

Table 3. Elemental chemical composition of sand.

Mass percentage (%)	SiO_2	Al_2O_3	CaO	MgO	Na_2O	K_2O	Fe_2O_3	TiO_2	Mn_2O_3	P_2O_5	BaO	SO_3	LOI
Sand	94.75	0.82	0.67	0.30	0	0	0.85	0.45	0	0	0	0	2.16

Table 4. Elemental chemical composition of Afagnan clay.

Mass percentage (%)	SiO_2	Al_2O_3	CaO	MgO	Na_2O	K_2O	Fe_2O_3	TiO_2	LOI
Clay	43.8	34.9	0.14	0.15	0.10	0.24	3.60	1.39	15.68

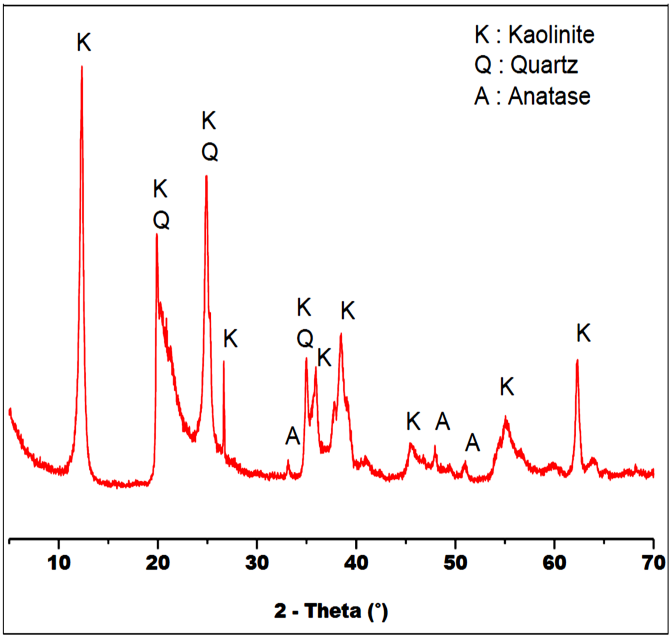


Figure 5. X-ray diffraction (XRD) of clay.

3.2. Characterization of the Developed Materials

1) Characterization of Materials Created Using the First Approach

The materials prepared using the first approach (**Figure 6**) were characterized by XRF spectroscopy (**Table 5**) and optical microscopy (**Figure 7**).

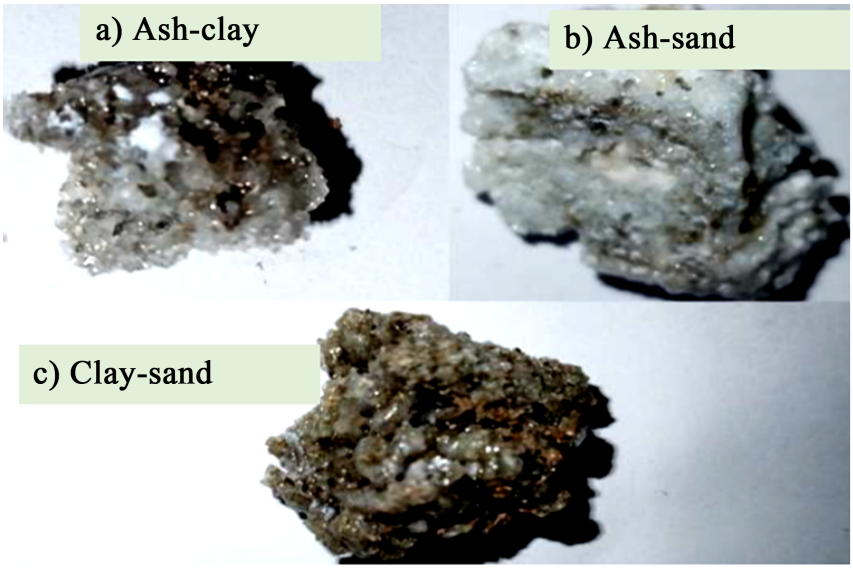


Figure 6. Image of the materials created using the first approach.

Table 5. Elemental chemical composition of the materials created using the first approach.

Mass percentage (%)	SiO_2	Al_2O_3	CaO	MgO	Na_2O	K_2O	FeO	Fe_2O_3	TiO_2	LOI
Ash-sand	51.8	12.31	20.56	6 .12	0.30	4.24	0	1.35	0.58	2.74
Ash-clay	40.46	28.54	10.43	4. 4	0.31	3.41	8.27	0	0.3	3.88
Clay-sand	54.43	29.23	0.21	0.18	0.11	0.23	12.67	0	0.14	2.8

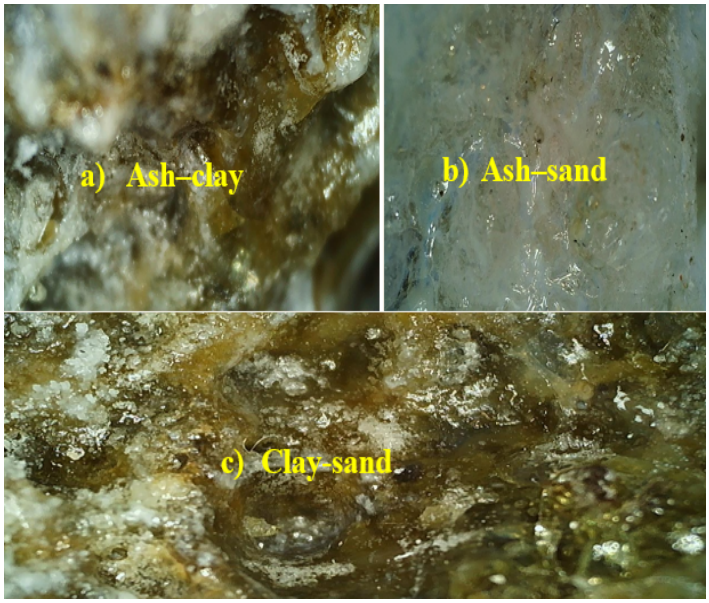


Figure 7. Optical micrograph of the surface of the materials created using the first approach.

2) Characterization of materials created using the second approach

For the materials prepared using the second approach, compressive strength tests (Table 6) and microscopic analysis (Figure 8) were performed.



Figure 8. Optical micrograph of the surface of the materials prepared using the second method.

Table 6. Results of uniaxial compressive strength tests.

	Composition of Materials (%)				Uniaxial compressive strength R_c (MPa)	Standard Deviation (MPa)	Coefficient of Variation (%)
	Clay	Sand	Ash	Lecithin			
M18	0	95	0	5	30.27	0.91	3.01
M16	13.67	79.33	2	5	28.74	0.5	1.74
M17	13.67	74	7.33	5	26.23	0.41	1.56
M13	13.67	65.67	15.66	5	25.49	0.47	1.84
M15	5.33	57.33	32.34	5	25.12	0.37	1.47
M14	13.67	57.33	24	5	24.81	0.99	3.99
M12	22	57.33	15.67	5	24.21	1.30	5.37
M11	27.77	52.85	14.38	5	23.86	1.02	4.27
M10	22	49	24	5	20.80	1.38	6.63
M9	30.33	32.33	32.34	5	19.70	0.84	4.26
M4	57	14	24	5	18.50	0.30	1.62
M3	62	14	19	5	17.60	0.49	2.78
M5	57	9	29	5	17.20	0.28	1.63
M2	72	9	14	5	16.80	0.81	4.82
M6	57	4	34	5	15.50	0.53	3.42
M1	82	4	9	5	15.10	0.42	2.78
M7	57	0	38	5	14.80	0.19	1.28
M8	95	0	0	5	14.40	0.23	1.60

Compressive strength tests were conducted on cubic bricks with a volume of 64 cm^3. The compressive strength value shown corresponds to the average compressive stress obtained from three specimens produced according to the same design protocol. The load was applied at a rate of 0.5 mm/min until its break, using an Instron universal testing machine (Model 3369) equipped with a compression force transducer with a maximum capacity of 50 kN. The specimens were dried at a laboratory room temperature (25˚C) for 24 hours prior to the compression test. The compressive strength is given by Equation 1.

$$R_c = F \Big/ \left(1600\ \text{mm}^2\right) \tag{1}$$

where, R_c: uniaxial compressive strength (MPa);

F: breaking load (N).

4. Results and Discussion

4.1. Raw Materials

The analysis of the raw materials revealed that the ash contains calcium oxide (70.11%), the sand contains silica (94.75%), while the clay contains 43.8% silica and 34.9% alumina, consisting mainly of kaolinite (Figure 5).

4.2. Materials Developed Using the First Approach

4.2.1. Microscopic Analysis

All of the newly obtained materials have a glassy, amorphous surface in various colors (Figure 7). There is also a complete absence of sand grains, indicating that the grains have completely fused. The material resulting from the ash-sand mixture has a whitish color, while those resulting from the ash-clay and clay-sand mixtures are white and dark green.

In order to better understand certain parameters, an elemental chemical characterization of the various materials was conducted.

4.2.2. Elemental Chemical Analysis

Elemental chemical analysis of the various materials revealed a high iron oxide content in the materials derived from the ash-clay and clay-sand mixtures, while the material derived from the ash-sand mixture had a high alumina content (Table 5). The coloration of the materials observed under a microscope is therefore due to the presence of iron and aluminum oxides.

In fact, ash and sand combined have a low alumina content, whereas the material obtained by their electroconsolidation using an electric arc plasma—generated by aluminum electrodes—contains a high percentage of alumina. This increase is therefore due to the oxidation of the aluminum electrodes in the plasma generator. Iron oxide (FeO) is also present in the materials (ash-clay and clay-sand) produced by plasma electroconsolidation using iron electrodes, whereas ash, sand, and clay do not contain it. These results confirm the oxidation of the metal electrodes in the plasma generator. In fact, to verify the influence of the type of electrodes on the composition of the materials, the electrodes were changed during the electroconsolidation of the various mixtures. This change in electrodes demonstrated that the type of electrodes could influence the composition of the resulting product.

4.3. Materials Developed Using the Second Approach

4.3.1. Microscopic Analysis

Examination of the surfaces of the new materials (Figure 8) revealed that materials M16, M17, and M18 had crack-free surfaces with well-bonded grains. An amorphous, slightly reflective substance was also observed on the surface of the materials; it could correspond to an intergranular cementation phase. These types of materials were obtained when the sand content was 74% or more of the mixture. Sand, therefore, acts as a binder in its amorphous form and helps bind or

cement the grains together. In fact, tests conducted as part of the initial study showed that the sand could melt at very low temperatures, ranging from 550 ˚C to 600 ˚C. Furthermore, when a small amount of ash rich in oxide (CaO) was added to the sand, it could melt completely at temperatures below 500˚C. Plasma therefore affects the melting temperature of materials. For the materials (M10, M11, M12, M13, M14, M15) with a sand content between 49% and 65.67%, partially fused grains, fused together with clearly visible pores, were observed under a microscope. A partial and non-uniform distribution of the amorphous phase, as well as the presence of cracks, was observed on the surface of the materials (M1, M2, M3, M4, M5, M6, M7, M8, M9), whose clay content ranged from 30.33% to 95%. Sand therefore interacts more readily with the plasma.

4.3.2. Uniaxial Compressive Strength (Rc)

Uniaxial compression strength tests (R_c) were conducted on all 18 composite material formulations developed using clay (from Afagnan), eucalyptus wood ash (SOPAL), sand (University of Lomé), and soy lecithin as the organic binder. The experimental results, including the average values (R_c), the standard deviations, and the coefficients of variation calculated based on 3 replicates by formulation, are summarized in Table 6. An analysis of the data in Table 6 reveals a wide range of mechanical strengths, ranging from 14.40 ± 0.23 MPa (formulation M8) to 30.27 ± 0.91 MPa (formulation M18). The standard deviation of all the series remains between 0.19 MPa and 1.38 MPa. More specifically, the coefficient of variation remains strictly below 7% (1.28% to 6.63%) for all the formulations tested. These low dispersion values confirm the excellent repeatability of the laboratory fabrication protocol as well as the satisfactory structural homogeneity of the blocks consolidated by electric arc plasma treatment.

The experimental results suggest that the electric arc plasma consolidation process exhibits high reactivity and a selective structural affinity for sand-rich matrices compared to clay-rich matrices. In fact, the M18 mixture (95% sand) achieves a maximum strength of 30.27 ± 0.91 MPa, while the M8 mixture (95% clay) develops only 14.40 ± 0.23 MPa. This selectivity can be explained, in part, by the ability of quartz grains to form solid fusion bridges under the influence of the plasma's heat flux, while the clay matrix undergoes rapid thermal shrinkage that can generate internal microcracks. Furthermore, the intergranular porosity of the sand facilitates the penetration of the energy flux and the uniform distribution of heat and ionized plasma species within the material, ensuring deeper and more effective consolidation.

5. Conclusions

This study evaluated the potential of electric arc plasma electroconsolidation using two different approaches. The first approach involved consolidating equiproportional mixtures of raw material powders (sand-ash, clay-ash, and clay-sand) by exposing them to a plasma flow. The second approach aimed to consolidate 18

cubic blocks of 64 cm^3 with different formulations by exposing each to the plasma flow. The experimental results related to the first approach highlighted two major phenomena, namely a high reactivity of the powder mixtures with the plasma flow, ensuring their consolidation in 15 minutes, as well as the solubilization of part of the metal electrodes within the plasma phase. The results of the second approach demonstrated, on the one hand, satisfactory structural homogeneity in the blocks consolidated by electric arc plasma treatment. On the other hand, they highlight a selective structural affinity of the plasma treatment toward matrices with a high sand content.

The results of this study lead us to conclude that electric arc plasma electroconsolidation holds immense potential for materials development. Nonetheless, despite confirming the effectiveness of this process, it remains crucial to evaluate its large-scale application for industrial purposes.

Author Contributions

Review and editing: Ablam Lazare AFANOU and K.C. Maurille Aziade. Supervision: Bassai Magnoudewa BODJONA and Diyakadola Diheenane BAFAI. Formal analysis: Sama OURO. Validation: Gado TCHANGBEDJI. Conceptualization, Methodology, Investigation, Writing: Ayi Kévin Ajavon. All authors have read and agreed to the published version of the manuscript.

Conflicts of Interest

The authors declare no conflicts of interest regarding the publication of this paper.

References

[1] Lewandowska, A., Sydor, M. and Bonenberg, A. (2025) A Review of Mycelium-Based Composites in Architectural and Design Applications. *Sustainability*, **17**, Article 11350. https://doi.org/10.3390/su172411350

[2] Holiarinala, V.M., Ramiharimanana, F.D., Rafanoela, H., Randriatsarazaka, S., Razafimahatratra, R., Metay, E., *et al.* (2025) Improvement of Malagasy Traditional Earth Bricks by Using a Derivative of CNSL as a Binding Agent. *ChemEngineering*, **9**, 22. https://doi.org/10.3390/chemengineering9020022

[3] Andrew, R.M. (2019) Global CO_2 Emissions from Cement Production, 1928-2018. *Earth System Science Data*, **11**, 1675-1710. https://doi.org/10.5194/essd-11-1675-2019

[4] Scrivener, K., Martirena, F., Bishnoi, S. and Maity, S. (2017) Calcined Clay Limestone Cements (LC3). *Cement and Concrete Research*, **114**, 49-56. https://doi.org/10.1016/j.cemconres.2017.08.017

[5] Habert, G., Miller, S.A., John, V.M., Provis, J.L., Favier, A., Horvath, A., *et al.* (2020) Environmental Impacts and Decarbonization Strategies in the Cement and Concrete Industries. *Nature Reviews Earth & Environment*, **1**, 559-573. https://doi.org/10.1038/s43017-020-0093-3

[6] Lachheb, M., Youssef, N. and Younsi, Z. (2023) A Comprehensive Review of the Improvement of the Thermal and Mechanical Properties of Unfired Clay Bricks by Incorporating Waste Materials. *Buildings*, **13**, Article 2314.

https://doi.org/10.3390/buildings13092314

[7] Zin, R.M., Soon, C.F., Sani, M.Z.A., Rizon, E.R., Tee, K.S., Ahmad, M.K., *et al*. (2017) Zero Voltage Switching Driver and Flyback Transformer for Generation of Atmospheric Pressure Plasma Jet. *AIP Conference Proceedings*, 1883, Article 020023. https://doi.org/10.1063/1.5002041